ELSEVIER

Fusion Engineering and Design 28 (1995) 716–723

Fusion Engineering and Design

Measurement techniques for fusion blanket neutronics experiments

Y. Oyama[a]*, C. Konno[a], Y. Ikeda[a], F. Maekawa[a], H. Maekawa[a], S. Yamaguchi[a], K. Tsuda[a], T. Nakamura[a], M.A. Abdou[b], E.F. Bennett[c], R.F. Mattas[c], K.G. Porges[c], M.Z. Youssef[b]

[a]*Department of Reactor Engineering, Tokai Research Establishment, Japan Atomic Energy Research Institute, Tokai-mura, Naka-gun, Ibaraki-ken 319-11, Japan*

[b]*Mechanical, Aerospace, and Nuclear Engineering Department, School of Engineering and Applied Science, University of California at Los Angeles, Los Angeles, CA 90024, USA*

[c]*Fusion Power Program Building 205, Argonne National Laboratory, 9700 South Cass Avenue, Argonne, Illinois 60439, USA*

Abstract

A variety of techniques to measure the nuclear parameters, such as tritium production rate, neutron spectrum, reaction rate and gamma-ray heating, in a simulated fusion blanket assembly have been developed or introduced through the JAERI/USDOE Collaborative Program on Fusion Blanket Neutronics. The features of those techniques are summarized and discussed with the experimental error. The present measurement techniques provided data with error ranges of 3–5% for tritium production, 5–10% for the neutron spectrum, 3–6% for the activation reaction and 10–20% for the gamma-ray heating rate.

1. Introduction

Techniques for the measurement of nuclear parameters are essential to perform a neutronics experiment. For fusion environments, neutron energy is higher than that of fission environments, and some of the parameters to be measured are also different from the case in fission reactor experiments. Thus, in the JAERI/USDOE Collaborative Program on Fusion Blanket Neutronics [1], many techniques have been developed or applied to measure nuclear parameters such as tritium production rate, neutron spectrum and reaction rate. Some of them are active (on-line) methods, taking the data at the same time as neutron irradiation, while the others are passive methods in which the data are taken after irradiation. The former require shorter measurement time with lower neutron intensity and thus can perform a number of experiments, while the latter require heavy (long and intense) neutron irradiation. The possibility of the desired experiments depends mostly on what kind of techniques can be applied. In this paper, the measurement techniques developed and applied are outlined and discussed, together with their features. These techniques are some of the most valuable results in the collaborative programs.

* Corresponding author.

SSDI 0920-3796(94)00311-4

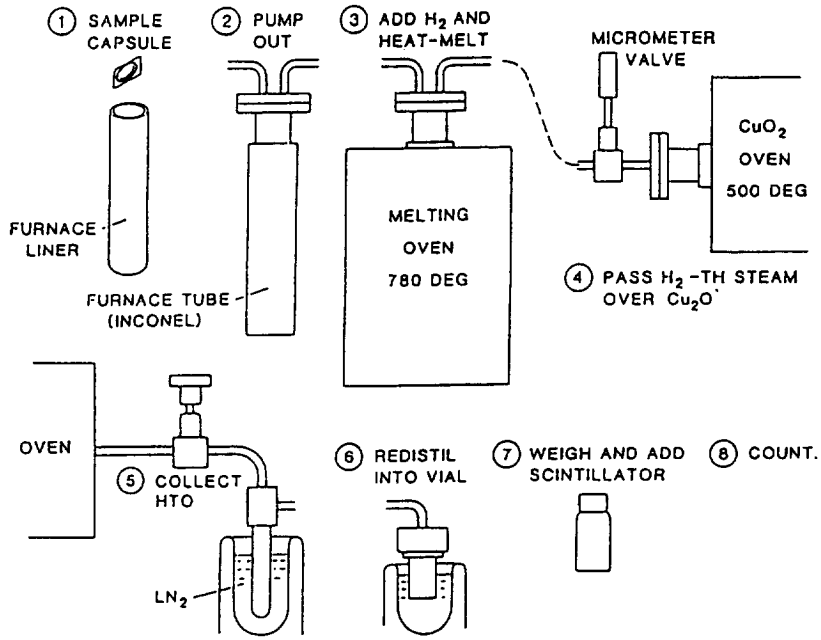

Fig. 1. Tritium extraction procedure for Li metal foil method.

This paper presents a review of the techniques used in the collaboration and discusses the status of them.

2. Techniques applied to nuclear parameter measurement

2.1. Tritium production rate (TPR)

2.1.1. Passive method

A passive method for tritium production rate measurements uses liquid scintillation counting techniques for tritium-containing solutions extracted from irradiated samples containing lithium. For this method, three kinds of probe materials (lithium metal foil, lithium oxide pellet and lithium oxide block) have been developed. The lithium metal foil method was originally developed by Bretscher [2] for a purpose other than fusion blanket evaluation, and adapted to the special needs of lithium oxide breeder blankets [3]. The Li metal sample size is 18 mm in diameter and 0.5 mm thick. The sample is encapsulated by aluminium and the outer diameter of the aluminium capsule is 23.8 mm. Fig. 1 shows the tritium extraction procedure for the Li metal foil method. Tritium is extracted from the samples by melting in a carrier hydrogen atmosphere and converted to HTO on a hot copper oxide surface. This gives the Bretscher method two advantages: first, no tritium escapes from the capsule during and just after irradiation; and second, all the extracted tritium is changed only to water form.

The method with Li_2O pellets is similar to the Li metal foil method except for the chemical process, but the advantage is to use the same material, Li_2O, as the material of the test blanket; no consideration is required of a self-shielding effect. The Li_2O pellet is a disc 20 mm in diameter and 3 mm in thickness. In order to expel 100% of tritium from irradiated sintered Li_2O pellets (weight ≈ 0.38 g, density $\approx 83\%$ of theoretical density), they were dissolved in water in a two-forked test tube. This way of resolving without acid avoids the background counts of scintillation by chemical luminescence.

The method with an Li_2O block to utilize the breeding materials piled as a mass to act as the detectors themselves was named the "zonal method" [4]. The zonal method is expected to have the following advantages, especially for heterogeneous configurations: (1) highly accurate data of the region-integrated tritium production rate can be obtained around the boundary of different materials, e.g. between beryllium and

lithium oxide, where the gradient of TPR distribution is very steep because it is free from positioning error, and (2) a good signal-to-background ratio can be obtained even in deep positions inside the test blanket, because of high sensitivity. Moreover, the first feature gives benchmark data suitable for Monte Carlo calculations, since zonal experimental data can be directly compared with the result of estimators of large volume such as track length estimators. Heating under vacuum is applied instead of the dissolution method for tritium extraction from irradiated bricks, and the detector can then be repeatedly used. The irradiated samples are heated to a temperature of 650 °C for 2 h. Tritium in the extracted gas is produced for each component of HTO and HT, and the amount tritium are measured. However, the HTO component was very small, i.e. 0.2–4%. The HT component was converted to HTO water by oxidation with a catalyser. Extracted tritiated water (6 cm^3) is mixed with 14 cm^3 of scintillation liquid, i.e. a total liquid sample of 20 cm^3 is prepared.

As with the other passive method, self-irradiation with LiF thermoluminescence dosimeters (TLDs) [5] was also applied to the tritium production rates of ^{6}Li, ^{7}Li and ^{N}Li. The LiF powder of TLD-600 (^{6}Li: 95.62 at.%), TLD-700 (^{7}Li: 99.993 at.%) and TLD-100 (natural abundance) purchased from Harshaw Chemical Co. Ltd, is sealed in 2 mm dia. × 12 mm Pyrex glass ampoules. The total neutron yield during the irradiation is typically 3.0×10^{16} n at the target. For 14 days after the neutron irradiation, to wait for the full decay of activated nuclei except for tritium, the TLDs are annealed at 400 °C for 2 h. After this process, they are kept in low background storage for 148 days. The thermoluminescence caused by the self-irradiation of β-rays from tritium during the storage period is measured by a TLD reader.

2.1.2. On-line method

An active (on-line) method is very useful when a quick measurement is required for many measuring points and for comparative study among experimental systems. For this purpose, the NE213 scintillation spectrometer is applied to obtain the tritium production rate (TPR). The threshold energy of the ^{7}Li(n,n'α)T reaction is about 3 MeV, while the measuring energy range of the NE213 is above 1 MeV. The TPR from ^{7}Li is estimated from the neutron spectrum measured by the NE213 spectrometer and the data of the ^{7}Li(n,n'α)T reaction cross-section. It should be noted that the TPR distributions obtained are biased by the cross-section data.

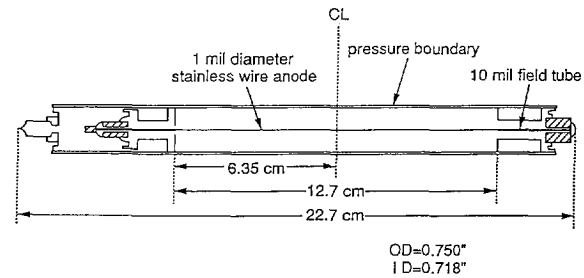

Fig. 2. Sectional view of small proton recoil gas proportional counter.

The tritium production rate (TPR) of ^{6}Li is also measured by using the difference between the response of the ^{6}Li glass scintillator (6-LGS) and that of ^{7}Li glass one (7-LGS) in a mixed neutron–gamma radiation field [6]. A peak caused by the ^{6}Li(n,α)T reaction appears on a Compton electron background produced by gamma-rays in the pulse height spectrum (PHS) of 6-LGS, while the 7-LGS detects mostly the gamma-ray background. By calculational analysis, the contribution of the charged particle emission reaction of ^{7}Li on the PHS was negligible. Since it can be assumed that the gamma-ray responses of both scintillators are almost identical, the gamma-ray background can be removed by subtracting the PHS of 7-LGS from that of 6-LGS. The total number of counts in the subtracted spectrum, which is equal to the total number of ^{6}Li(n,α)T events in the scintillator, corresponds to the tritium production rate of ^{6}Li. For the case of a thin scintillator, in addition to the PHS subtraction the correction of the edge effect (distortion of pulse height due to the wall escape of alpha and/or triton) is taken into account [7]. However, corrections for flux perturbation are neglected, because our scintillator is thin enough to neglect the self-shielding effect.

2.2. In-system neutron spectrum

A detector for in-system neutron spectrometry basically requires the following characteristics: (1) the detector should be made as small as possible so as to reduce the perturbation due to the detector and so as to obtain good spatial resolution; (2) the response of the detector must be irrespective of the incident direction of neutrons; and (3) gamma-rays associated with DT neutrons can be rejected. Two types of miniature detector measuring proton recoil spectrum have been developed.

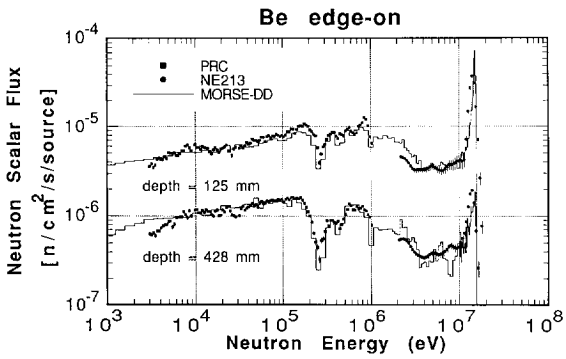

Fig. 3. Examples of the measured neutron spectra inside the simulated blanket, together with the calculated ones [1].

2.2.1. Small sphere NE213 scintillation detector

A small spherical detector with an NE213 liquid scintillator was developed to measure the neutron spectrum inside the test blanket at energies of several hundred keV to 15 MeV [8]. A 14 mm diameter spherical NE213 liquid scintillator is used as a probe for neutron detection. An NE213 liquid of 1.38×10^3 mm^3 is contained in a spherical cell of Pyrex glass of 1 mm thickness. Two pulse height spectra with different gains are combined around 2 MeV proton energy and unfolded by the FORIST program [9] using the neutron response matrix. The response matrix is calculated separately by Monte Carlo method, in which the responses in specially important energy regions, i.e. 13.6–14.8 MeV, are replaced by the responses directly measured with a d-T neutron source. Also, the absolute efficiency is normalized with the absolute neutron flux determined by the associated alpha-particle counting technique.

2.2.2. Small proton recoil gas proportional counter

A small gas proportional counter with hydrogen gas was developed by Bennett to cover energies of a few keV to 2 MeV [10]. The counter body is fabricated from 0.41 mm thick 304SS alloy. The inner diameter and the effective length are 18.2 mm and 127 mm, respectively, as shown in Fig. 2. To encompass the neutron spectrum over the energy range from 1 keV to 1 MeV, two different gas fillings are used for identical counters, hydrogen at 5.5 atm with 1% CH_4 for the low-energy component, and an 8.8 atm 50:50 mixture of hydrogen and argon for the upper energy component. Argon increases the stopping power, thereby reducing the proton recoil range. The neutron detecting efficiency is given by the number of hydrogen atoms and the elastic cross-section. A high-voltage supply with ramped sweep to perform the simultaneous measurement with different gains was developed instead of several separate runs with different applied voltages [11]. Signals from the counter are fed to both the "fast" and "slow" amplifiers, which correspond the rise time information and the energy, respectively, and neutron pulses are discriminated by the rise time window. The neutron energy spectrum is derived by unfolding the pulse height spectrum using the differential method. Fig. 3 shows the typical results of neutron spectrum obtained from both NE213 and the proton recoil gas proportional counter (PRC) with the results calculated by the Monte Carlo transport program.

2.3. Foil activation technique

This passive dosimeter method has, in general, several advantages: (1) the activation technique is well established; (2) the responses of the activation detectors have been well studied and evaluated in the dosimetry files; (3) the small size of the detector foil makes for good spatial resolution and less perturbation of the field; and (4) the neutron spectrum can be deduced by using multiple foil detectors with different responses even though the energy resolution is poor. In Table 1, selected reactions are listed with their effective threshold energies. In particular, the general use of common dosimetry reactions, e.g. ^{27}Al(n,α)^{24}Na, ^{56}Fe(n,p)^{56}Mn, ^{58}Ni(n,p)^{58}Co, ^{58}Ni(n,2n)^{57}Ni, ^{90}Zr(n,2n)^{89}Zr, ^{93}Nb(n,2n)^{92m}Nb, ^{115}In(n,n')^{115m}In, ^{197}Au(n,γ)^{198}Au, over all the experimental systems, provided beneficial neutronics information for systematic analysis through comparative study concerning material and geometrical configurations.

The foils are irradiated typically for about 10 h with D-T neutrons and total neutron yields at the target are 4.3×10^{16} n for the irradiation run using experimental drawer channels. After irradiation, gamma-rays from the irradiated foils are measured in parallel with several Ge detectors.

2.4. Gamma-ray heating rate

2.4.1. Interpolation method by thermoluminescent dosimeters

The measurements of gamma-ray heating using thermoluminescent dosimeters (TLD) were performed for the fast breeder reactor mock-up experiments, but there has been no measurement for fusion neutrons. The interpolation method for gamma-ray heating measurement using TLDs proposed by Tanaka et al. [12] was applied to the experiments. The relation between the absorbed dose in a medium and that in a TLD is written as

Table 1
Dosimetry reactions

Reactions	Half-life	Abundance × γ-ray branching ratio (%)	Threshold energy (MeV)
$^{27}Al(n,\alpha)^{24}Na$	15.02 h	100.0	5
$^{n}Ti(n,x)^{46}Sc$	83.83 d	99.98	4
$^{n}Ti(n,x)^{47}Sc$	3.341 d	68.0	1.5
$^{n}Ti(n,x)^{48}Sc$	1.821 d	100.0	5
$^{55}Mn(n,\gamma)^{56}Mn$	2.579 h	98.9	—
$^{54}Fe(n,p)^{54}Mn$	312.2 d	5.8	2
$^{56}Fe(n,p)^{54}Mn$	2.579 h	90.71	5
$^{58}Ni(n,p)^{58}Co$	70.92 d	67.92	2
$^{58}Ni(n,2n)^{57}Ni$	1.503 d	53.18	12.5
$^{59}Co(n,\alpha)^{56}Mn$	2.579 h	98.9	6
$^{59}Co(n,2n)^{58}Co$	70.92 d	99.5	10
$^{64}Zn(n,p)^{64}Cu$	12.70 h	36.06	1.5
$^{90}Zr(n,2n)^{89}Zr$	3.268 d	50.94	12
$^{93}Nb(n,2n)^{92m}Nb$	10.15 d	99.0	9
$^{115}In(n,n')^{115m}In$	4.486 h	43.83	0.34
$^{197}Au(n,\gamma)^{198}Au$	2.694 d	95.5	—
$^{197}Au(n,2n)^{196}Au$	6.183 d	87.0	8.5

$$D_m = f(\mathrm{M,TLD},E_\gamma)^{-1} D_{\mathrm{TLD}} \quad (1)$$

where D_m is the absorbed dose in a medium M, D_{TLD} is the absorbed dose in a TLD, $f(\mathrm{M,TLD},E_\gamma)$ is a conversion factor and E_γ is the gamma-ray energy. According to Tanaka et al., an absorbed dose in a TLD overestimates that in the surrounding medium with an atomic number smaller than that of the TLD, while it underestimates for the opposite case. In addition, the measured values of TLDs increase monotonically with atomic number. Thus, the absorbed dose in a medium can be obtained as an interpolated or extrapolated value at the atomic number of the medium of interest, when the measured values of TLDs are plotted with the effective atomic number of TLD. The great advantage of this method is that it does not require any gamma-ray spectrum information. However, the neutron contribution should be subtracted with the aid of a calculation. Fig. 4 shows the calculated neutron response for each TLD [13]. The neutron contribution is usually large at the front of the test blanket. Measurements are performed with four kinds of TLD: ^{7}LiF(Mg), Mg_2SiO_4(Tb), Sr_2SiO_4(Tb) and Ba_2SiO_4(Tb).

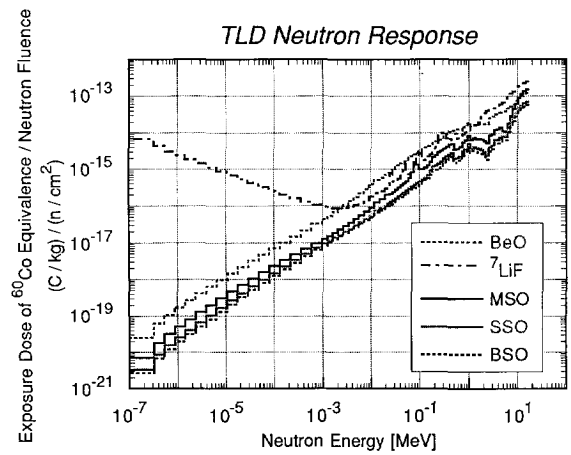

Fig. 4. Calculated neutron responses of various TLDs. The abbreviations MSO, SSO and BSO stand for Mg_2SiO_4, Sr_2SiO_4 and Ba_2SiO_4, respectively.

2.4.2. Spectrum weighting function method with NE213 detector

The spectrum weighting function method [14] was developed to measure an in-system gamma-ray heating rate distribution at the same time as the measurement of the neutron spectrum using the NE213 scintillation detector. The NE213 scintillation detector can separate the gamma-ray response from the neutron response, and the gamma-ray response of the detector gives the energy information. The kerma factor of gamma-rays is obtained from the mass energy absorption coefficient,

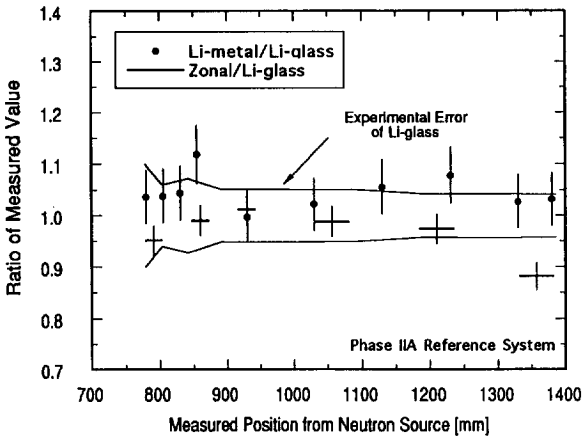

Fig. 5. Comparison of the results of the ^{6}Li tritium production rate measured by different techniques in the lithium oxide test blanket.

so that the gamma-ray heating rate H is obtained using the following function

$$H = \int K(E_\gamma)\Phi(E_\gamma)\mathrm{d}E_\gamma \tag{2}$$

where $K(E_\gamma)$ is the kerma factor of the surrounding material and $\Phi(E_\gamma)$ is the photon flux with energy E_γ.

The photon flux is related to the recoil electron spectrum by the response matrix R of the scintillator. The spectrum weighting function relates the recoil electron spectrum to the integrated value without explicit use of the response matrix, $R(E_\gamma,E_e)$. By using the spectrum weighting function, $G(E_e)$, the heating rate is represented as

$$H = \int C(E_e)G(E_e)\mathrm{d}E_e \tag{3}$$

where $C(E_e)$ is an electron energy spectrum measured by the NE213 scintillator, and $G(E_e)$ is determined so as to satisfy the relation

$$K(E_\gamma) = \int R(E_\gamma,E_e)G(E_e)\mathrm{d}E_e \tag{4}$$

From the above relation, the gamma-ray heating rate is obtained by the small NE213 scintillation detector, assuming that the detector does not perturb the gamma field. To obtain the spectrum weighting function, first the gamma-ray response is calculated by the Monte Carlo program and renormalized to the measured response by using a standard gamma-ray source. Second, the weighting function is determined by solving the integral Eq. (4) using a successive approximation method, such as the SAND-II program.

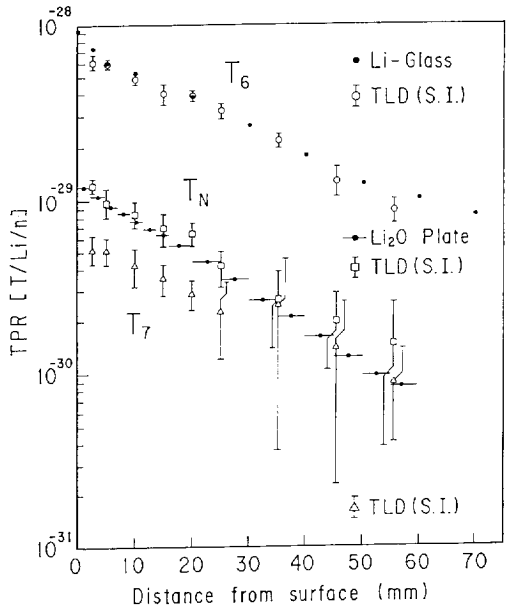

Fig. 6. Tritium production rate measured by the TLD self-irradiation method with Li-glass and zonal (Li_2O plate) methods. The symbol S.I. denotes the TLD self-irradiation method.

3. Discussion

3.1. Tritium production rates

3.1.1. Liquid scintillation counting techniques

Error contributions due to statistics of counting can usually be eliminated except for the inherent uncertainty of background averaging. To clarify the ambiguity in the tritium escape in the form of recoiled tritons, pellets sandwiched with aluminium foils are irradiated near the neutron source. The ratio of tritium escaped from the pellets is 1.1%. The estimated errors in common with scintillation counting techniques are due to the atomic number of Li, weighing and scintillation counting efficiency, and the total becomes 3% after correction. However, taking account of the self-shielding correction and signal-to-background ratio, additional errors of a few percent, depending on neutron spectrum and fluence, are necessary, except for the zonal method with natural Li_2O block, which is free from self-shielding and has high sensitivity. Fig. 5

shows the comparison of the results from the Li metal foil and zonal methods with the result from the Li glass method. The figure indicates good agreements between them.

3.1.2. Self-irradiation method with TLDs

The TPR data of ^{6}Li (T_6) are corrected for atomic ratios of ^{6}Li and ^{7}Li in the TLD-600. The TPR distributions of TLD are shown in Fig. 6 with those of the Li glass and Li_2O zonal methods. As the TPR distributions of TLD are not measured absolutely, the data for T_6 at 48.8 mm in the figure are normalized to 6.0×10^{-29} (arbitrary value) and the other TLD data are shifted relatively.

3.1.3. On-line method

Systematic errors come mainly from the source neutron yield and atomic number of ^{6}Li. The ^{6}Li atom number in the ^{6}Li glass scintillator is determined by isotope dilution analysis within an uncertainty of $\approx 0.5\%$. Random errors are due to the statistical error of ^{6}Li(n,α)T reaction counting of 0.3–1.1%. The error of the fitting method in the pulse height subtraction is estimated by the maximum variation of the peak area due to statistical error.

3.2. Neutron spectrum

For the NE213 spectrometer, the accuracy of the neutron response in the neutron energy range of 13.6 to 14.8 MeV is about 2% from the experimental confirmation. However, the errors of the higher energy neutron responses are accumulated for errors in the lower energy range, because the response error of 2% is still large. In addition, the calculated light output response corresponding to the proton energy below about 2 MeV gives a relatively poor representation due to mixing of the alpha-particle response from carbon reactions by high-energy neutrons. Therefore the error of the unfolded spectrum in the range below the 14 MeV peak is attributed to the mismatch of the used response in the case that 14 MeV neutrons are dominant. If the flux above 10 MeV is, for example, ten times larger than the flux below 10 MeV, the uncertainty of proton spectra in the range 6 to 10 MeV might become -10% to -20% at maximum. The energy calibration error also affects the unfolded results. The effects of a variation of 2% in the energy axis are $\approx 3\%$ above 10 MeV and less than 2% for the 1–10 MeV range, respectively. The overall error comes to 4% for the flux above 10 MeV and 10–20% below 10 MeV, depending on the neutron spectrum to be measured.

For the proton gas proportional counter technique, possible error sources are the gas pressure (hydrogen atomic number), n-p scattering cross-section, the fitting error for differentiation of the recoil proton spectrum due to count statistics, and calibration of recoil energy. They are expected to be less than 1% for each of the first two items and usually about 10% for the rest. Moreover, the influence of the wall-end effect in the upper energy region and the ambiguity of ionization energy (W value) in the lower energy region should be accounted for. For each energy point in the obtained flux, the overall error is expected to be around 3–10%.

3.3. Reaction rate with activation foils

Major sources of errors for the reaction rate are the gamma-ray counting statistics (0.1% to several percent) and the detector efficiency (2–3%). The error for sum-peak correction is estimated to be less than 2%, depending on the decay mode and fraction of the multiple gamma-ray cascade. The error for the decay correction is reflected from the error in the half-life of the activity. If the half-life is accurate, the error for the saturation factor should be less than 1% even for short half-life activities. The other errors, associated with foil weight, gamma-ray self-absorption, irradiation time, cooling time and counting time, are negligibly small. The overall error of reaction rate ranges from 3% to 6%.

3.4. Gamma-ray measurement

For the TLD method, the experimental errors are due to a dispersion of the TL measurement of 2–15%, gamma-ray response calibration of 2–10%, neutron response subtraction of 10–20% and interpolation of less than 20%. Finally, the overall error is 20–30%.

For the spectrum weighting function method, the error is estimated by the uncertainties of source neutrons, weighting function, gamma-ray response matrix and the kerma factor. The error of the response matrix is assumed to be 20% for systematic errors. The error of the kerma factor is assumed to be 10% for systematic errors. The error of the weighting function is estimated from the range of results obtained by different iterations and a systematic error of 5–50% is obtained for each weighting function. These errors propagate to the error in the gamma-ray heating rate by 10% from the first two sources and 3–10% from the weighting function, respectively. Finally, the overall error becomes 5–15%, excluding the detector perturbation.

4. Concluding remarks

The present measurement techniques provided data with an error range of 3–5% for tritium production, 5–10% for the neutron spectrum, 3–6% for the activation reaction and 10–20% for the gamma-ray heating rate. Consequently, the measurement techniques for an engineering benchmark have been established by these series of collaborative experiments. In fusion reactor development, the error ranges obtained indicate the present limitation of experimental confirmation of the design parameters. For example, it is difficult to confirm the tritium production rate within 3% accuracy, so that it gives a lower limit for confirmation of accuracy of the design calculation.

For a future experiment, most of the present techniques could not be applied to measurements in a fusion device where high temperatures and high magnetic fields exist. The active method has a problem due to electric components and insulators. The scintillators do not work at such high temperatures. The gas counter needs research and development for high-temperature duty and magnetic field effect. The passive method of tritium production also does not work at high temperature because of tritium escape. At present, only a foil activation technique can work under fusion device conditions without any modification. Thus the development of new techniques is needed for nuclear technology experiments in fusion reactors such as ITER.

Acknowledgment

The US contributions were supported by the US Department of Energy, Office of Fusion Energy.

References

[1] T. Nakamura and M.A. Abdou, Summary of recent results from the JAERI/US fusion neutronics Phase I experiment, Fusion Technol., 10 (1986) 541; Y. Oyama, K. Tsuda, S. Yamaguchi, Y. Ikeda, C. Konno, H. Maekwa, T. Nakamura, K.G. Porges, E.F. Bennett and R.F. Mattas, Experimental results for Phase II of the JAERI/USDOE collaborative program on fusion blanket neutronics, Fusion Eng. Des., 9 (1989) 309; Y. Oyama, C. Konno, Y. Ikeda, H. Maekawa, F. Maekawa, K. Kosako, T. Nakamura, A. Kumar, M.Z. Youssef and M.A. Abdou, Phase III experimental results of the JAERI/USDOE collaborative program on fusion blanket neutronics experiments, Fusion Eng. Des. 18 (1991) 203.

[2] M.M. Bretscher and W.C. Redman, Nucl. Sci. Eng. 39 (1970) 368.

[3] K.G. Porges and M.M. Bretscher, Breeding rate measurements in solid fusion blankets with metallic lithium samples, Fusion Technol. 19 (1991) 1903.

[4] K. Tsuda, Japan Atomic Energy Research Institute, personal communication, 1985.

[5] H. Maekawa, A method for obtaining the tritium production rate distribution with a tritium production rate distribution with a LiF thermoluminescence dosimeter, JAERI-M 6055, Japan Atomic Energy Research Institute (In Japanese); UCRL-TRANS-11196 (1979).

[6] S. Yamaguchi, Y. Oyama, T. Nakamura and H. Maekawa, An on-line method for tritium production measurement with a pair of lithium-glass scintillators, Nucl. Instrum. Meth. A254 (1987) 413.

[7] S. Yamaguchi, Edge effect of thin lithium-glass scintillators, Nucl. Instrum. Meth. A274 (1989) 573.

[8] Y. Oyama, S. Tanaka, K. Tsuda, Y. Ikeda and H. Maekawa, A small spherical NE213 scintillation detector for use in in-assembly fast neutron spectrum measurement, Nucl. Instrum. Meth. A256 (1987) 333.

[9] FORIST spectrum unfolding code: Radiation Shielding Information Center, Oak Ridge National Laboratory, PSR-92 (1975).

[10] E.F. Bennett and T.J. Yule, Techniques and analyses of fast reactor neutron spectroscopy with proton-recoil proportional counters, ANL-7763, Argonne National Laboratory (1971).

[11] E.F. Bennett, A continuous mode data acquisition technique for proton recoil proportional counter neutron spectrometers, ANL/FPP/TM-239, Argonne National Laboratory (1989).

[12] S. Tanaka and N. Sasamoto, Gamma-ray absorbed dose measurements in media with plural thermoluminescent dosimeters having different atomic numbers, J. Nucl. Sci. Technol. 22 (1985) 109.

[13] S. Yamaguchi, H. Maekawa, K. Kosako and T. Nakamura, Measurements of gamma-ray heating in lithium-oxide, graphite and iron slab assemblies bombarded by D-T neutrons, Fusion Eng. Des. 10 (1989) 163.

[14] Y. Oyama and S. Tanaka, Neutron dosimeter based on a spectrum weighting function method using an NE213 scintillation detector, JAERI-M 9982 (1982) (in Japanese).